Indian Journal of Chemistry
Vol. 57A, January 2018, pp. 9-17

Calcium oxalate crystallization in SDS solutions

Yan Li[a], Xifeng Lu[b], Xiaodeng Yang[a,]* & Yulin Wang[c]

[a]Key Laboratory of Fine Chemicals (Shandong Province), Qilu University of Technology, Ji'nan 250353, PR China

[b]Lunan Institute of Coal Chemical Engineering, Jining 272000, PR China

[c]College of Jining Polytechnic, Ji'ning 272000, PR China

Email: yangxiaodeng@qlu.edu.cn

Received 1 November 2017; revised and accepted 15 December 2017

Sodium dodecyl sulfate (SDS) and hydroxy isopropyl chitosan (HPCHS) are employed as modulation agents for crystallization of CaC_2O_4. The effects of concentrations of SDS and HPCHS, $[Ca^{2+}]/[C_2O_4^{2-}]$, $[Mg^{2+}]/[Ca^{2+}]$ and ratio of $V_{ethanol}/V_{water}$ and $[Mg^{2+}]/[Ca^{2+}]$ on the crystallization are investigated. The CaC_2O_4 particles are characterized by scanning electron microscopy, powder X-ray diffraction, thermogravimetric analysis, and Fourier transform infrared spectroscopy. The results show that SDS inhibits the crystallization and growth of CaC_2O_4 particles due to the interaction between dodecyl sulfate and Ca^{2+} and also the formation of calcium dodecyl sulfate. Based on an analysis of the CaC_2O_4 and solution properties of SDS/Ca^{2+} and HPCHS/SDS/Ca^{2+}, a mechanism for CaC_2O_4 crystallization in SDS solutions is proposed. This work is of significance in inhibiting abnormal mineralization.

Keywords: Crystallization, Calcium oxalate, Sodium dodecyl sulfate, Hydroxy isopropyl chitosan

An organism contains more than 60 kinds of minerals, which exist in the form of inorganic and organic compounds. The minerals have certain intensity and toughness due to the precisely controlled morphologies, shapes and sizes[1]. These minerals also show various special biological functions, for instance, calcium carbonate could be a physical barrier to harmful organisms and microorganisms. Calcium phosphates also a synthetic bone graft substitutes for their osteoconductive and appropriate mechanical strength.

Biomineralization is the process of formation of biominerals with special structures and assemblies under the modulation of biomacromolecules. During the process, the inorganic minerals are formed and assembled through the interaction between biomacromolecules and inorganic mineral particles[2]. There are two kinds of biomineralization processes: one is the normal mineralization process, in which the metal ions not only take part in the formation of some bioactive complexes, but also take part in the formation of hard tissues, such as bone, and teeth. The other is the abnormal mineralization process in which various internal or external factors interfere with the normal mineralization, resulting in unbalanced mineralization, like the formation of calculus, hardening of the arteries, bone hyperplasia, the plaque and dental caries, and so on[1,3]. Among various calculi, the dissoluble calcium salts account for about 73%, and more than 80% dissoluble calcium salts are calcium oxalates. For instance, calcium oxalate mineralized in urinary system is the main component of calculi[3].

Calcium oxalate includes three polymorphs: calcium oxalate monohydrate ($CaC_2O_4 \cdot H_2O$, COM), calcium oxalate dihydrate ($CaC_2O_4 \cdot 2H_2O$, COD) and calcium oxalate trihydrate ($CaC_2O_4 \cdot 3H_2O$, COT). The above sequence of the three polymorphs shows the decreasing order in thermodynamic stability. Calcium oxalates mainly exist in COM or COD polymorph[4].

The crystallization and properties of calcium oxalate have been extensively studied in various organic additives, such as amino acids/proteins[5-8], phospholipids[9,10], surfactants[11], polymers[12], and magnesium ions[13]. Siddiqui *et al.*[14] revealed that myeloperoxidase and calcium granule proteins promoted the aggregation of calcium oxalate crystals since these anti-inflammatory proteins were adsorbed on the surfaces of calcium oxalate, and became the

internal templates during the crystallization process. Ouyang *et al.*[4,15] found that the perfect Langmuir-Blodgett (LB) film of dipalmitoylphosphatidylcholine only induced a small amount of COM particles. However, the damaged LB film induced circle-shaped COM. The results indicated the important relationship between kidney stones and the damaged adrenal film at the molecular level.

Vesicle, double sealed structure formed by directional bilayer of amphiphilic molecules, is one of the optimal candidates for researching and simulating biological membranes[16]. Hao *et al.*[17] synthesized well-dispersed and elongated hexagonal shaped COM with vesicles as micro-reactors. They found that the growth rate of the (020) plane increased with the increase in Ca^{2+} concentration. Amino acids, pH, added surfactant, and the type of microemulsions showed significant impact on the morphologies of calcium oxalate[6,7].

Sodium dodecyl sulfate (SDS) is one of the typical anionic surfactants, widely used in protein separation[18], pharmaceutical delivery[19,20], dispersion of carbon nanotubes[21], and inorganic materials synthesis[22,23]. In this study, SDS was employed to modulate calcium oxalate crystallization. The effects of concentrations of SDS and HPCHS, $[Ca^{2+}]/[C_2O_4^{2-}]$, ratio of $V_{ethanol}/V_{water}$ and $[Mg^{2+}]/[Ca^{2+}]$ on the crystallization were investigated. To investigate the role of HPCHS and SDS in modulating the crystallization of CaC_2O_4, the aqueous properties of HPCHS/SDS/Ca^{2+} and SDS/Ca^{2+} mixtures were studied by surface tension method. Based on an analysis of the CaC_2O_4 and properties of SDS/Ca^{2+} and HPCHS/SDS/Ca^{2+} solutions, a crystallization mechanism of CaC_2O_4 in SDS solutions is proposed. The work is of significance in inhibiting abnormal mineralization.

Materials and Methods

Hydroxy isopropyl chitosan (HPCHS) was synthesized according to literature method[24]. Sodium dodecyl sulfate (SDS, molecular biological grade) was obtained from Promega Co. $CaCl_2$, $MgCl_2 \cdot H_2O$, $Na_2C_2O_4$, and anhydrous ethanol were all A.R. grade, obtained from the Tianjin Tianda Purification Material Fine Chemical factory, and used without further purification. Triply distilled water was used in the preparation of all solutions.

Crystallization and characterization of CaC_2O_4 particles

Aqueous solutions of HPCHS (3.0 g/L), SDS (10 mmol/L), $CaCl_2$ (200 mmol/L) and $Na_2C_2O_4$ (200 mmol/L) were prepared as stock solutions. In a typical experiment, a solution of $Na_2C_2O_4$ (0.5 mL, 200 mmol/L) was dropped into a solution of SDS (2.0 mL, 10 mmol/L) and $CaCl_2$ (0.5 mL, 200 mmol/L) with 17 mL of triply distilled water in an element bottle under mild stirring. Thus, the initial concentration of SDS was 1.0 mmol/L and those of Ca^{2+} and $C_2O_4^{2-}$ were 0.5 mmol/L each. Unless indicated otherwise, the calcium oxalate particles were collected by centrifugation after 5 h, washed with triply distilled water three times and then dried in a vacuum desiccator at 40 ºC for 24 h.

The morphology and particle size of the calcium oxalate particles were characterized by a JEOL JSM6700F field-emission scanning electron microscope (FE-SEM) fitted with a field emission source and operated at an accelerating voltage of 5 kV. X-ray diffraction (XRD) patterns were recorded on a Rigaku D/max-2200PC diffractometer with graphite-monochromatized high-intensity Cu-K_α radiation (λ = 1.5406 Å, 40 kV, 40 mA). A scan rate of 0.02° steps/(25 s) and a 2θ range from 20° to 60° were selected. Fourier transform infrared (FTIR) spectroscopic measurements were recorded on a Bruker Equinox 55 spectrometer.

Surface tension of SDS/Ca^{2+} and HPCHS/SDS/Ca^{2+} solutions

To investigate the crystallization mechanism of CaC_2O_4 in SDS solution, the surface tension of SDS/Ca^{2+} (or HPCHS/SDS/Ca^{2+}) mixed solutions was measured on a K12 processor tensiometer (Krüss Co. Germany) by the ring method at 25±1 ºC.

Results and Discussion

Crystallization of CaC_2O_4 in solutions with or without SDS

To analyze the effect of SDS on CaC_2O_4 crystallization, CaC_2O_4 was crystallized in solutions with or without (control experiment) 1.0 mmol/L SDS at 40 ºC. The plate-like CaC_2O_4 particles (Fig. 1a) with length of ~500 nm and width of ~175 nm were obtained in the control experiment, but the aggregated cylindrical crystals (Fig. 1b) with length of ~350 nm and diameter of ~180 nm were obtained in 1.0 mmol/L SDS solution at the aging time of 1 h. As the aging time increased to 5 h, the side lengths of CaC_2O_4 particles (Fig. 1c) crystallized in the control experiment increased to ~640 nm (long side) and ~220 nm (short side). In the solutions with SDS, the length of cylindrical crystals increased to ~440 nm and the diameter increased to ~220 nm (Fig. 1d). The volume of the CaC_2O_4 particles crystallized in

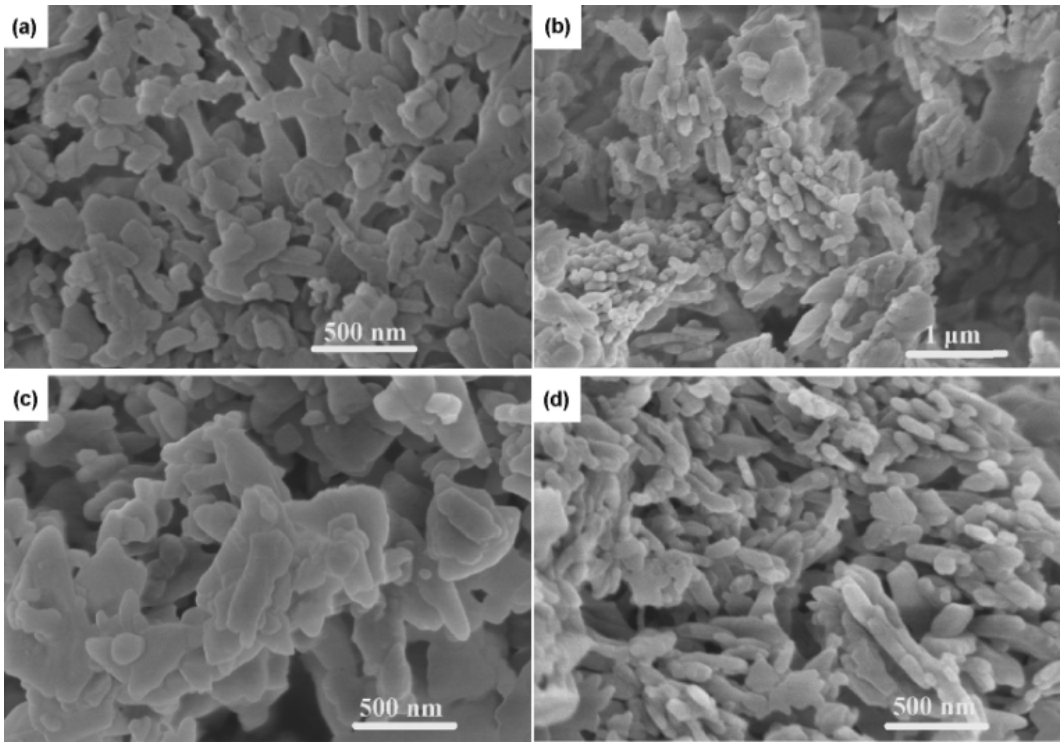

Fig. 1 — Typical SEM images of CaC_2O_4 particles crystallized in solutions without (a and c) and with (b and d) SDS at 40 °C. [Conc. of Ca^{2+} and CO_3^{2-}: 5.0 mmol/L each, SDS: 1.0 mmol/L; aging time: 1 h (a and b) or 5 h (c and d)].

1.0 mmol/L SDS solution is much smaller than that crystallized in control experiment due to the electrostatic interaction between SDS and Ca^{2+}, as well as the formation of calcium dodecyl sulfate (CDS)[25], which acts as a template and inhibits the growth of CaC_2O_4.

Figure 2 shows the XRD patterns of CaC_2O_4 particles crystallized in the control experiment (curves 1 and 3) and in solutions with 1.0 mmol/L SDS (curves 2 and 4) at different aging time. The CaC_2O_4 particles are all hydrated calcium oxalate (COM), and the lattice parameters are a = 0.63, b = 0.73, c = 0.99 nm (JCPDS 33-0268). The values of surface spacing (d) are 0.595, 0.365, 2.97 and 2.36 nm, corresponding to (101), (020), (202) and (130) surfaces, respectively. The peak intensities of (101) and (020) surfaces as well as their ratios are listed in Table 1. The peak intensity of (020) surface for CaC_2O_4 crystallized in control experiment is far stronger than that for CaC_2O_4 crystallized in solutions with SDS. However, the ratio of I_{101}/I_{020} for CaC_2O_4 crystallized in SDS solutions is much larger than that of CaC_2O_4 crystallized in control experiment. The SEM images show that SDS inhibits the growth of CaC_2O_4 and the inhibiting effect on (020) surface is more notable than that on (101) surface.

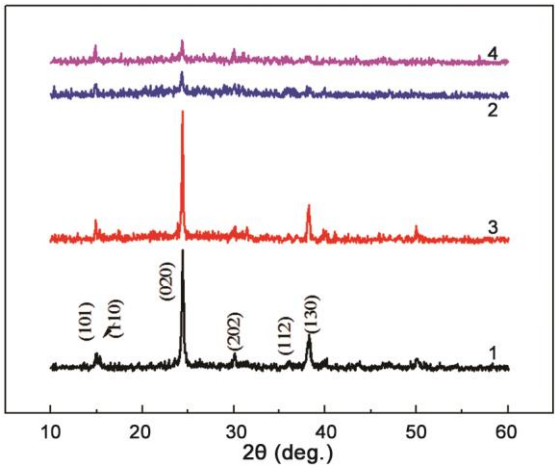

Fig. 2 — XRD patterns of CaC_2O_4 particles crystallized in solutions without SDS (curves 1 and 3) and with SDS (curves 2 and 4). [The samples correspond to those in Fig. 1].

The FTIR spectra of the CaC_2O_4 particles confirm the formation of COM (Fig. 3). The absorption peaks at 948 and 665 cm^{-1} are the characteristic absorption peaks of COM. The peaks at 1614 and 1319 cm^{-1} are the asymmetric and symmetric absorption peaks of COO^-, respectively, while the peaks at 783 and 519 cm^{-1} are the bending absorption peaks of O-C-O, out-of-plane and in-plane respectively, and the peaks

Table 1 — Diffraction intensities of (101) and (020) surfaces, and the values of I_{101}/I_{020} for CaC_2O_4 particles crystallized in different systems

System	I_{101}	I_{020}	I_{101}/I_{020}
Control (Water)	16.85[a]	137.46	0.12
	23.60[b]	152.02	0.16
SDS	11.09[a]	25.13	0.44
	17.22[b]	23.11	0.74
HPCHS	22.56[b]	184.67	0.12
HPCHS/SDS	23.28[b]	146.56	0.16
$[Ca^{2+}]/[C_2O_4^{2-}]$	14.86[c]	21.02	0.71
	16.36[d]	30.42	0.54
$V_{ethanol}/V_{H_2O}$	28.60[e]	27.67	1.03
	17.67[f]	25.82	0.69
	13.02[g]	17.91	0.73
	12.82[h]	15.86	0.81
$[Mg^{2+}]/[Ca^{2+}]$	9.26[i]	13.10	0.71
	28.75[j]	49.83	0.58
	6.70[k]	5.11	1.31

[a]Aging time: 1 h; [b]5 h. [c]$[Ca^{2+}]/[C_2O_4^{2-}]$: 1:4; [d]4:1. [e]$V_{ethanol}/V_{H_2O}$: 1:4; [f]1:3; [g]1:2; [h]1:1. [i]$[Mg^{2+}]/[Ca^{2+}]$: 1:4; [j]1:1; [k]4:1.

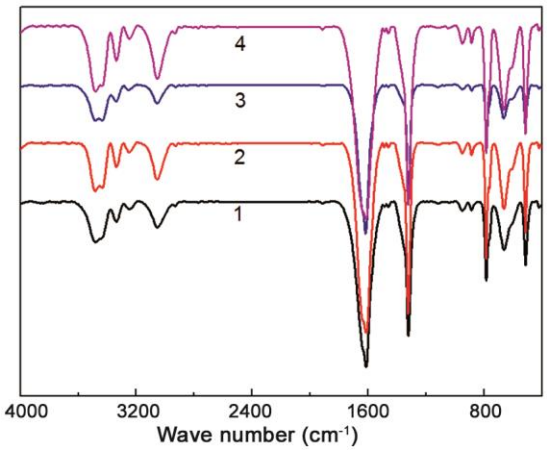

Fig. 3 — FTIR spectra of CaC_2O_4 crystals crystallized in solutions without SDS (a and c) and with SDS (b and d) SDS. [The samples correspond to those in Fig. 1].

at 3000-3500 cm^{-1} are the asymmetric and symmetric vibration absorption peak of bound water[26].

Effect of HPCHS on CaC_2O_4 crystallization

Polysaccharide is an important organic compound widely distributed in animals and microorganisms. It is involved in various activities of cell life, including the mineralization process. In recent years, the polysaccharide controlled growth of inorganic crystals has attracted much attention[27]. Chitosan is one of the most important polysaccharides, with several attractive features, such as low price, rich resources, biocompatibility, biodegradation, and low toxicity[28-31]. However, its water insolubility inhibits wide applications. Many studies focused on the modification of chitosan to improve the solubility and other physicochemical properties are reported[32-34]. In previous studies, several chitosan derivatives were synthesized and employed to modulate the $CaCO_3$ crystallization[24,35-37]. HPCHS is one of the most important functional chitosan derivatives, and can form liquid crystals. HPCHS solution has excellent foam performance, emulsification capability[38,39], anticoagulant activity, antimicrobial activity and clinical effects[40,41]. Based on its excellent performance in medical and clinical applications, HPCHS was selected to control CaC_2O_4 crystallization with SDS to explore its inhibiting effect on urinary calculus.

Figure 4 shows the SEM images of CaC_2O_4 crystallized in HPCHS (1.0 g/L) and HPCHS (1.0 g/L)/SDS (1.0 mmol/L) mixed solutions at varying aging time. It can be seen that the particles crystallized in HPCHS solution have random morphologies due to the electrostatic interaction of $–NH_2$ in HPCHS on the positively charged surfaces of CaC_2O_4. The small, irregular flaky structured particles are crystallized in HPCHS (1.0 g/L)/SDS (1.0 mmol/L) mixed solution after 1 h aging time. When aging time is increased, the irregular flaky particles increase. This change indicates that the addition of HPHCS in SDS solution weakens the effect of SDS on the growth of CaC_2O_4 particles; the interaction between SDS and HPCHS weakens the impact of SDS on CaC_2O_4. On the other hand, HPCHS has the potential to promote the growth of CaC_2O_4 flaky particles, which is proved by XRD patterns (Fig. S1, Supplementary Data). The peak intensity of (020) surface for CaC_2O_4 particles crystallized in HPCHS is significantly stronger than that for CaC_2O_4 particles crystallized in control experiment (Table 1). Both XRD patterns and FTIR spectra (Figs S1 and S2, Supplementary Data) prove that the crystals are all COM.

Effect of $[Ca^{2+}]/[C_2O_4^{2-}]$ ratio on CaC_2O_4 crystallization

In some systems, the amounts of Ca^{2+} and $C_2O_4^{2-}$ are not the same, indicating that the concentration of Ca^{2+} or $C_2O_4^{2-}$ may affect CaC_2O_4 crystallization. Therefore, it is necessary to investigate the effect of $[Ca^{2+}]/[C_2O_4^{2-}]$ratio on CaC_2O_4 crystallization while the concentration of SDS is 1.0 mmol/L.

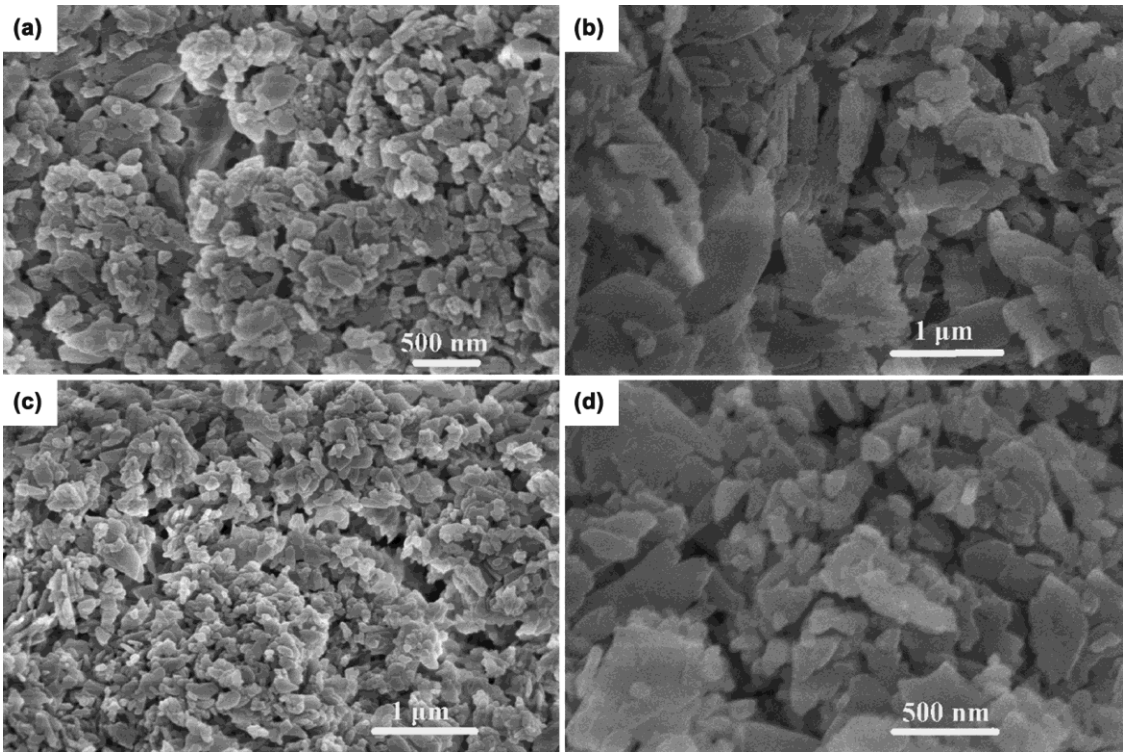

Fig. 4 — Typical SEM images of CaC_2O_4 crystallized in solutions with HPCHS (a and b) and with HPCHS/SDS (c and d). [Aging time: 1 h (a and c) and 5 h (b and d). Conc. of HPCHS: 1.0 g/L, and, SDS: 1.0 mmol/L].

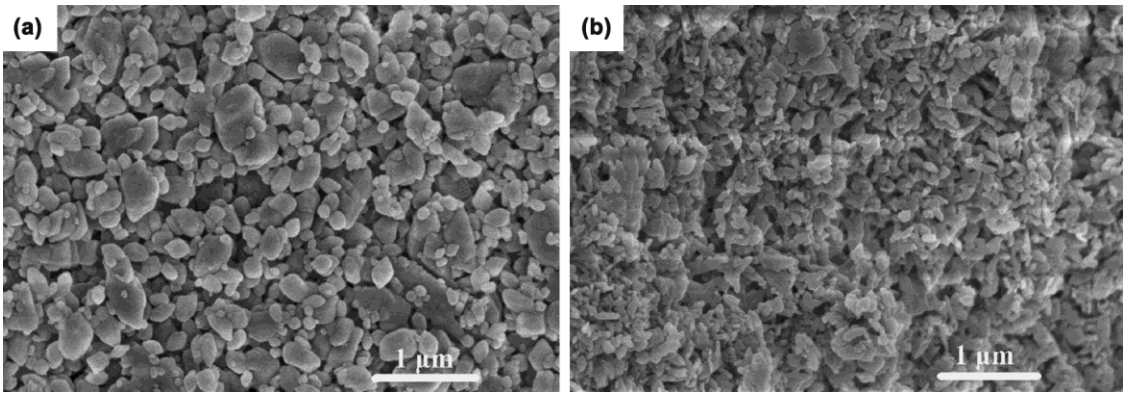

Fig. 5 — Typical SEM images of CaC_2O_4 crystallized in solutions with $[Ca^{2+}]/[C_2O_4^{2-}]$ ratio of (a) 1:4, and, (b) 4:1.

Typical SEM images of CaC_2O_4 crystallized in solutions with 1.0 mmol/L SDS and $[Ca^{2+}]/[C_2O_4^{2-}]$ ratio of 1:4 and 4:1 are shown in Fig. 5. At $[Ca^{2+}]/[C_2O_4^{2-}]$ ratio of 1:4, hexagonal CaC_2O_4 particles with long diagonal of ~410 nm and short diagonal of ~220 nm are obtained (Fig. 5a). At $[Ca^{2+}]/[C_2O_4^{2-}]$ratio of 4:1, irregular small plate particles are obtained (Fig. 5b). A similar observation was reported during the heterogeneous nucleation process of $CaCO_3$[42]. When Ca^{2+} is in excess, the excessive Ca^{2+} ions are adsorbed on the surfaces of precipitated particles, preventing the heterogeneous nucleation and growth of irregular particles. In addition, the solubility of calcium oxalate increases with the increase in Ca^{2+} concentration[43]. On the other hand, the CO_3^{2-} ions promote the heterogeneous nucleation of $CaCO_3$[42]. Therefore, the CaC_2O_4 particles crystallized in solutions with $[Ca^{2+}]/[C_2O_4^{2-}]$ ratio of 1:4 are larger than those crystallized in solutions with $[Ca^{2+}]/[C_2O_4^{2-}]$ ratio of 4:1.

Both XRD patterns and FTIR spectra of the obtained CaC_2O_4 indicate that the CaC_2O_4 particles

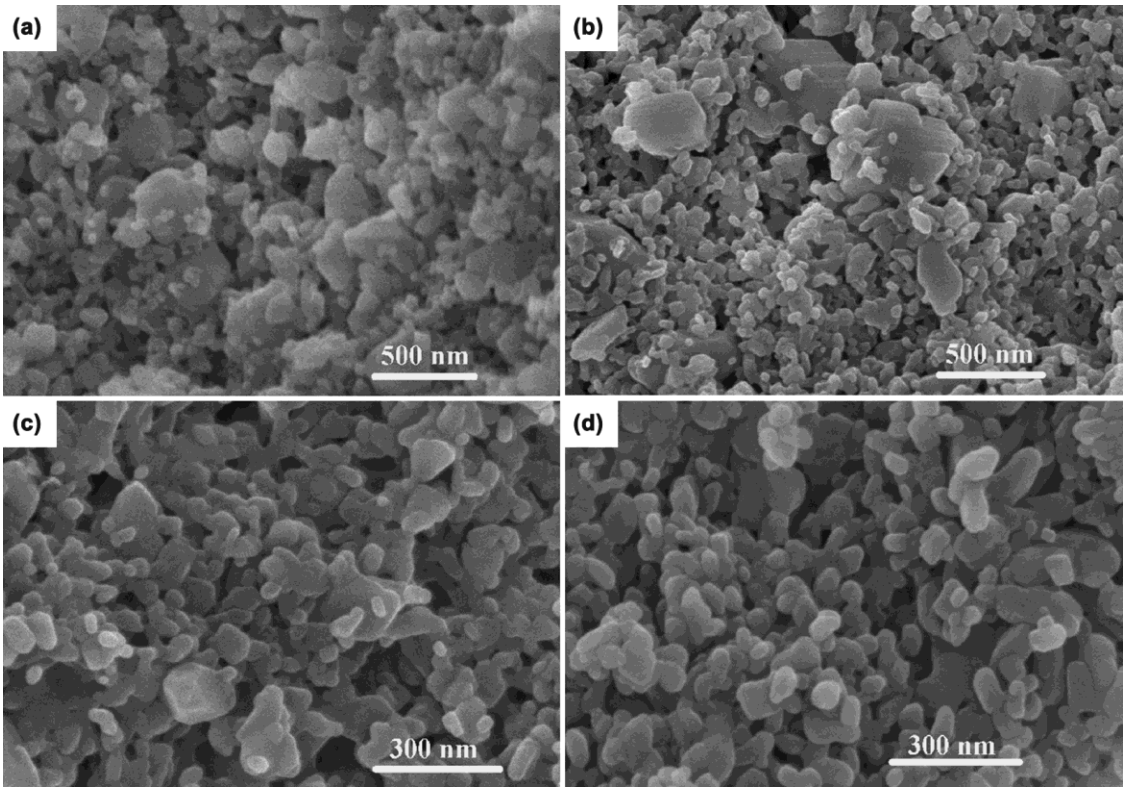

Fig. 6 — Typical SEM images of CaC_2O_4 crystallized in ethanol/water mixed solutions. [$V_{ethanol}/V_{H2O}$ = 1:4 (a), 1:3 (b), 1:2 (c) and 1:1 (d)].

are all COM (Figs S3 & S4, Supplementary Data). The peak intensities of (101) surface for CaC_2O_4 crystallized at the $[Ca^{2+}]/[C_2O_4^{2-}]$ratios of 1:4 and 4:1 are almost the same. However, the peak intensity of (020) surface for CaC_2O_4 crystallized at $[Ca^{2+}]/[C_2O_4^{2-}]$ ratio of 4:1 is slightly stronger than that for CaC_2O_4 crystallized at $[Ca^{2+}]/[C_2O_4^{2-}]$ ratio of 1:4. The ratio of I_{101}/I_{020} for CaC_2O_4 crystallized at $[Ca^{2+}]/[C_2O_4^{2-}]$ ratio of 4:1 is also larger than that for CaC_2O_4 crystallized at $[Ca^{2+}]/[C_2O_4^{2-}]$ ratio of 1:4 (Table 1). The difference is caused by the growth promoting effect of $C_2O_4^{2-}$ on single crystal as well as the accumulation of Ca^{2+}. This is consistent with that observed from SEM images.

Effect of ethanol on the crystallization of CaC_2O_4

The effect of ethanol on CaC_2O_4 crystallization and growth were investigated at 40 °C, keeping the volume ratios of ethanol-to-water as 1:4, 1:3, 1:2, and 1:1 (Fig. 6(a-d)). Typical SEM images of CaC_2O_4 show that the CaC_2O_4 particles (~220 nm ($V_{ethanol}/V_{H2O}$=1:4), 150 nm (1:3), 100 nm (1:2), 80 nm (1:1) in length) crystallized in ethanol are much smaller than those crystallized in the solutions containing HPCHS (~720 nm) (or HPCHS/SDS, ~400 nm) (Fig. 4). With the increase of ethanol content from 1:4 to 1:3 to 1:2 to 1:1, the average CaC_2O_4 particle size decreases significantly from 200 nm to 100 nm to 65 nm to 60 nm, indicating that ethanol inhibits CaC_2O_4 growth. This change may be ascribed to the miscibility of ethanol and water as well as the variation of mixed solvent properties.

The XRD patterns and FTIR spectra show that the CaC_2O_4 particles are COM (Figs S5 & S6, Supplementary Data). The addition of ethanol in water decreases CaC_2O_4 peak intensity, and the peak intensity decreases with the increase of the ($V_{ethanol}/V_{H2O}$) ratio. The value of I_{101}/I_{020} increases gradually with the increase in ($V_{ethanol}/V_{H2O}$) (Table 1), suggesting that the ethanol mainly inhibits the growth of the (020) surface. The XRD results are similar to that observed from SEM images.

Effect of Mg^{2+} on CaC_2O_4 crystallization

Mg^{2+} is an indispensable metal ion in organisms and may affect the crystallization of biominerals in organisms. Therefore, the effect of Mg^{2+} on CaC_2O_4 crystallization was investigated, keeping the ratios of $[Mg^{2+}]/[Ca^{2+}]$ as 1:4, 1:1, and 4:1.

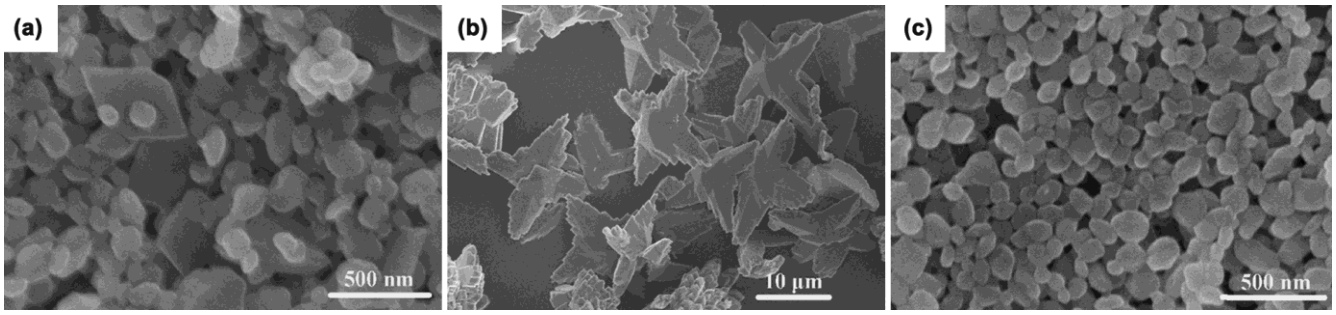

Fig. 7 — Typical SEM images of CaC_2O_4 particles crystallized at $[Mg^{2+}]/[Ca^{2+}]$ ratios of (a) 1:4, (b) 1:1, (c) 4:1.

Figure 7 shows that the addition of Mg^{2+} affects the morphology of CaC_2O_4 particles significantly. Spherical particles were crystallized at $[Mg^{2+}]/[Ca^{2+}]$ ratios of 1:4 and 4:1, and the average size of the particles crystallized at $[Mg^{2+}]/[Ca^{2+}]$ ratio of 1:4 (~120 nm) is larger than that of the particles crystallized at the ratio of 4:1 (~100 nm). In addition, there are small amounts of tetrahedral particles crystallized in the system with $[Mg^{2+}]/[Ca^{2+}]$ of 1:4. The star-like particles with long side of ~5 μm were crystallized at $[Mg^{2+}]/[Ca^{2+}]$ of 1:1. This observation is very interesting and will be systematically researched in subsequent work.

During the crystallization of CaC_2O_4, Mg^{2+} ions control COM precipitation and growth dynamically[44], promoting the formation of calcium oxalate dehydrate (COD). During the crystallization of COD, magnesium oxalate was also crystallized[45] and induced excessive adsorption or precipitation of COD due to the low solubility of magnesium oxalate[14,44]. XRD patterns and FTIR spectra confirm the formation of COD (Figs S7 & S8, Supplementary Data).

Mechanism of CaC_2O_4 crystallization in SDS solution

To explore the mechanism of CaC_2O_4 crystallization in SDS solution, the surface tensions of SDS, SDS/$CaCl_2$ (0.5 mmol/L), and HPCHS (1.0 g/L)/SDS/$CaCl_2$ (0.5 mmol/L) solutions were measured (Fig. 8). For solutions of SDS and HPCHS (1.0 g/L)/SDS/$CaCl_2$ (0.5 mmol/L), one breakpoint was observed in the surface tension versus SDS concentration plot. The breakpoint corresponds to the critical micelle concentration (cmc). However, there is a sudden-increase-point in the surface tension curve of SDS/$CaCl_2$ solution. Generally, inorganic salts affect the aggregation behavior of surfactant from two aspects: (i) inorganic salt compresses the electrical double layer surrounding the hydrophilic groups and decreases the cmc of surfactant and, (ii) inorganic salts

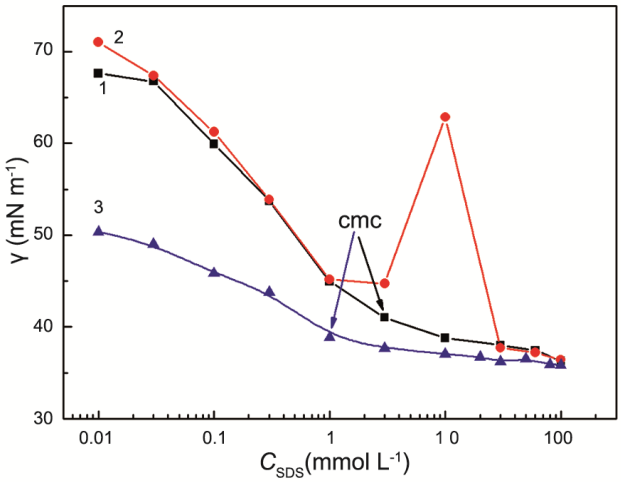

Fig. 8 — Surface tension plots versus SDS concentration in solutions (a) without $CaCl_2$, (b) with $CaCl_2$, and, (c) with HPCHS/$CaCl_2$.

change the ionic strength of the solutions and increase surfactant activity[16]. In this experiment, the addition of $CaCl_2$ showd (i) no effect on the activity of SDS due to the interaction between Ca^{2+} and dodecyl sulfate ions (DS^{2-}), and, (ii) the formation of calcium dodecyl sulfate (CDS), which is insoluble in water at room temperature. The sudden-increase-point at 10 mmol/L Ca^{2+} and the FTIR spectra (Fig. S9, Supplementary Data) confirm the formation of CDS. The result of conductivity also proves the formation of CDS[28].

In this study, the optimum concentration of SDS was 1.0 mmol/L, corresponding to the formation of CDS pre-micelles, which modulate the formation of the aggregated cylindrical CaC_2O_4 crystals. The addition of HPCHS in SDS solution favors the interaction between SDS and HPCHS[46-48], inhibits the formation of CDS, and promotes the crystallization and growth of CaC_2O_4 particles.

Conclusions

The effects of SDS, HPCHS, $[Ca^{2+}]/[C_2O_4^{2-}]$, $V_{ethanol}/V_{H2O}$ and $[Mg^{2+}]/[Ca^{2+}]$ on CaC_2O_4 crystallization have been investigated. SDS inhibits CaC_2O_4 crystallization and growth significantly through electrostatic interaction between DS^{2-} and Ca^{2+}. On the other hand, HPCHS promotes the growth of CaC_2O_4 (020) surface due to the adsorption of $–NH_2$ groups. Both Ca^{2+} and $C_2O_4^{2-}$ inhibit the growth of (020) surface remarkably when their concentrations are not the same, but show slight influence on (101) surface growth. Ethanol inhibits the growth of the (101) and (020) surfaces and its inhibitory effect increases with increasing $V_{ethanol}/V_{H2O}$. Mg^{2+} ions induce the formation of spherical COD when the ratios of $[Mg^{2+}]/[Ca^{2+}]$ are 1:4 and 4:1, while the cruciate-flowered COD is induced when the ratio of $[Mg^{2+}]/[Ca^{2+}]$ is 1:1. The aqueous properties of SDS/Ca^{2+} solution indicate that the electrostatic interaction between SDS and Ca^{2+} ions and the formed CDS plays a key role in CaC_2O_4 crystallization.

Supplementary Data

Supplementary data associated with this article are available in the electronic form at http://www.niscair.res.in/jinfo/ijca/IJCA_57A(01)9-17_SupplData.pdf.

Acknowledgement

This work was undertaken with the financial support from National Natural Science Foundation of China (grant No. 21306092), Science and Technology Plan Project of Shandong Provincial University (grant no. J12LA02) and Program for Scientific Research Innovation Team in Colleges and Universities of Shandong Province.

References

1 Mann S, *Biomineralization: Principles and Concepts in Bioinorganic Materials Chemistry*, (Oxford University Press, UK) 2001, pp. 6-23.
2 Bunker B C, Rieke P C, Tarasevich B J, Campbell A A, Fryxell G E, Graff G L, Song L, Liu J, Virden J W & McVay G L, *Science*, 264 (1994) 48.
3 Ouyang J M, *J Funct Mater*, 36 (2005) 173.
4 Deng S P & Ouyang J M, *Cryst Growth Des*, 9 (2009) 82.
5 Shen Y, Li S, Xie A, Xu W, Qiu L, Yao H, Yu X & Chen Z, *Colloids Surf B*, 58 (2007) 298.
6 Shen Y, Yue W, Xie A, Li S & Qian Z, *Colloids Surfaces B*, 45 (2005) 120.
7 Wang L, Qiu S R, Zachowicz W, Guan X, DeYoreo J J, Nancollas G H & Hoyer J R, *Langmuir*, 22 (2006) 7279.
8 Grohe B, O'Young J, Ionescu D A, Lajoie G, Rogers K A, Karttunen M, Goldberg H A & Hunter G K, *J Am Chem Soc*, 129 (2007) 14946.
9 Ouyang J M & Deng S P, *Colloids Surf A*, 317 (2008) 155.
10 Talham D R, Backov R, Benitez I O, Sharbaugh D M, Whipps S & Khan SR, *Langmuir*, 22 (2006) 2450.
11 Sikirić M, Filipović-Vinceković N, Babić-Ivančić V, Vdović N & Füredi-Milhofer H, *J Colloid Interf Sci*, 212 (1999) 384.
12 Akyol E & Öner M, *J Crystal Growth*, 307 (2007) 137.
13 Wright E R & Delaune R H, *Ind Eng Chem Anal Ed*, 18 (1946) 426.
14 Mushtaq S, Siddiqui A A, Naqvi Z A, Rattani A, Talati J, Palmberg C & Shafqat J, *Clin Chim Acta*, 384 (2007) 41.
15 Ouyang J M, *Chem*, 65 (2002) 326.
16 Zhao G X & Zhu B Y, *Surfactant Action Principle* (China Light Industry Press, Beijing) 2003, pp. 291-295.
17 Teng M, Song A, Liu L & Hao J, *J Phys Chem B*, 112 (2008) 1671.
18 Schägger H & von Jagow G, *Anal Biochem*, 166 (1987) 368.
19 Sharma P, Bhardwaj V, Chaudhary T, Sharma I, Kumar P & Chauhan S, *J Mol Liq*, 187 (2013) 287.
20 Hadjmohammadi M & Salary M, *J Chromatogr B*, 912 (2013) 50.
21 Blanch A J, Quinton J S & Shapter J G, Carbon, 60 (2013) 471.
22 Yang C, Song X, Sun S, Sun Z & Yu J, *Adv Powder Technol*, 24 (2013) 585.
23 Rezaei-Sameti M, Nadali S, Falahatpisheh A & Rakhshi M, *Solid State Commun*, 159 (2013) 18.
24 Yang X, Xu G, Chen Y, Wang F, Mao H, Sui W, Bai Y & Gong H, *J Crystal Growth*, 311 (2009) 4558.
25 Shen Q, Wang L, Huang Y, Sun J, Wang H, Zhou Y & Wang D, *J Phys Chem B*, 110 (2006) 23148.
26 Ali A M, Raj N A N, Kalainathan S & Palanichamy P, *Mater Lett*, 62 (2008) 2351.
27 Ouyang J M, *Biomineralization's Matrix Control And Biomimetic Applications*, (Chemical Industry Press, Beijing) 2006, pp. 55-56.
28 Sui W, Huang L, Wang J & Bo Q, *Colloid Surf B*, 65 (2008) 69.
29 Sui W, Wang Y, Dong S & Chen Y, *Colloid Surf A*, 316 (2008) 171.
30 Hu Y, Wang M, Wang D, Gao X & Gao C, *J Membr Sci*, 319 (2008) 5.
31 Lin A, Liu Y, Huang Y, Sun J, Wu Z, Zhang X & Ping Q, *Int J Pharm*, 359 (2008) 247.
32 Zeng J B, He Y S, Li S L & Wang Y Z, *Biomacromol*, 13 (2012) 1.
33 Kumar M N V R, *React Funct Polym*, 46 (2000) 1.
34 Friedman M & Juneja A K, *J Food Prot*, 73 (2010) 1737.
35 Yang X, Xu G, Chen Y, Liu T, Mao H, Sui W, Ao M & He F, *Powder Technol*, 204 (2010) 228.
36 Yang X, Xu G, Chen Y & Sui W, *Powder Technol*, 215-216 (2012) 185.
37 Yang X, Meng H, Li T, Shi L, Li Y & Xu G, *Powder Technol*, 256 (2014) 272.
38 Dong Y, Wu Y, Wang J & Wang M, *Eur Polym J*, 37 (2001) 1713.

39 Sui W, Fan J, Yang X & Chen G, *Polym Mater Sci Eng*, 19 (2003) 109.

40 Wang A, Xiao Y, Cao N, Jia B & Xue Z, *Chinese J Biochem Pharmaceut*, 18 (1997) 16.

41 Peng Y, Han B, Liu W & Xu X, *Carbohyd* Res, 340 (2005) 1846.

42 Fang W, *Control the Synthesis of Inorganic Minerals with the Method of Amphiphilic Molecule Soft Template* (Ph.D Thesis, Shandong University) 2006, pp. 62-64.

43 Doherty W O S, *Ind Eng Chem Res*, 45 (2006) 642.

44 Desmars J F & Tawashi R, *BBA-Gen Subjects*, 313 (1973) 256.

45 Liebman M & Costa G, *J Urology*, 163 (2000) 1565.

46 Sunintaboon P, Pumduang K, Vongsetskul T, Pittayanurak P, Anantachoke N, Tuchinda P & Durand A, *Colloid Surf A*, 414 (2012) 151.

47 Onesippe C & Lagerge S, *Carbohydr Polym*, 74 (2008) 648.

48 Onesippe C & Lagerge S, *Colloid Surf A*, 317 (2008) 100.